Analytica Chimica Acta 875 (2015) 92–98

Contents lists available at ScienceDirect

Analytica Chimica Acta

journal homepage: www.elsevier.com/locate/aca

Sensitive colorimetric assays for α-glucosidase activity and inhibitor screening based on unmodified gold nanoparticles

Hongxia Chen [a], Jiangjiang Zhang [a], Heng Wu [a], Kwangnak Koh [b], Yongmei Yin [c,*]

[a] Laboratory of Biosensing Technology, School of Life Sciences, Shanghai University, Shanghai 200444, PR China
[b] Institute of General Education, Pusan National University, Pusan 609-735, Republic of Korea
[c] Department of Oncology, The First Affiliated Hospital of Nanjing Medical University, Nanjing 210029, PR China

HIGHLIGHTS

- A novel colorimetric strategy for α-glucosidase activity assay and inhibitor screening has been established.
- The sensing strategy relies on triple-catalyzation amplification and unmodified gold nanoparticles as signal material.
- An excellent sensitivity with detection limit of 0.001 U mL^{-1} (α-glucosidase) was obtained.

GRAPHICAL ABSTRACT

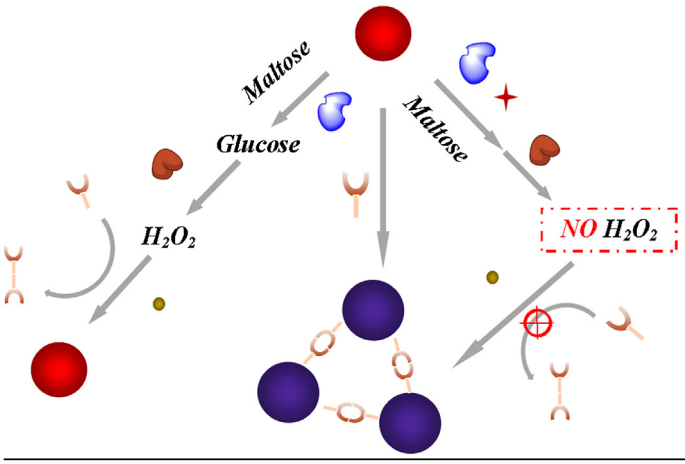

ARTICLE INFO

Article history:
Received 25 December 2014
Received in revised form 3 February 2015
Accepted 10 February 2015
Available online 12 February 2015

Keywords:
Colorimetric biosensor
Gold nanoparticle
α-Glucosidase
Inhibitor

ABSTRACT

A colorimetric sensor has been developed in this work to sensitively detect α-glucosidase activity and screen α-glucosidase inhibitors (AGIs) utilizing unmodified gold nanoparticles (AuNPs). The sensing strategy is based on triple-catalytic reaction triggered by α-glucosidase. In the presence of α-glucosidase, aggregation of AuNPs is prohibited due to the oxidation of cysteine to cystine in the system. However, with addition of AGIs, cysteine induced aggregation of AuNPs occurs. Thus, a new method for α-glucosidase activity detection and AGIs screening is developed by measuring the UV–vis absorption or visually distinguishing. A well linear relation is presented in a range of 0.0025–0.05 U mL^{-1}. The detection limit is found to be 0.001 U mL^{-1} for α-glucosidase assay, which is one order of magnitude lower than other reports. The IC_{50} values of four kinds of inhibitors observed with this method are in accordance with other reports. The using of unmodified AuNPs in this work avoids the complicated and time-consuming modification procedure. This simple and efficient colorimetric method can also be extended to other enzymes assays.

* Corresponding author. Tel.: +86 25 68136043; fax: +86 25 68136043.
E-mail address: ym.yin@hotmail.com (Y. Yin).

http://dx.doi.org/10.1016/j.aca.2015.02.022
0003-2670/

1. Introduction

Diabetes has become one of the most suffering chronic diseases with highly substantial incidence around the world. Diabetes consists of three main types: type I, type II and gestational diabetes. Globally, type II diabetes is the most common type among the three categories. It almost accounts for 90% of all diabetics. Moreover, type II diabetes mellitus is associated with an increased risk of both cardiovascular and neurological diseases in the development of diabetes [1–4]. α-Glucosidase inhibitors (AGIs) are the main targets in the early treatment and prevention of diabetes. AGIs play a very important role in controlling the patients' postprandial blood glucose levels and keeping glucose levels within a relatively normal range [5,6]. Therefore, it is of great significant to develop sensitive and easily operated methods to determine α-glucosidase activities and screen α-glucosidase inhibitors for finding new and effective oral medicines of type II diabetes.

Currently, several methods have been developed for detection of α-glucosidase activity and its inhibitors screening. Generally, two approaches are employed: *in vivo* screening (the animal model of hyperglycemia); *in vitro* screening (enzyme-inhibitor model) [7–10]. The *in vivo* animal model provides more reliable results and is critical for the clinical assessment. However, it involves long-term lasting experiments and is relatively expensive. So, the *in vitro* enzyme-inhibitor model, using *para*-nitrophenyl-α-D-glucopyranoside (PNPG) as artificial substrate, has also been widely employed. Nevertheless, although the PNPG-based methods offer a relatively simple approach to assay α-glucosidase activity and screen AGIs, their sensitivity is limited to some extent, because the effect of AGIs is quantified by recording absorbance of 4-nitrophenol released from PNPG [11]. For even worse case, the assessment is interfered when the overlaps of absorption happens between AGIs and 4-nitrophenol [12].

Colorimetric assay is a widely employed approach for different assays due to its simplicity and practicality, in addition to the electrochemical methods [13–16]. Especially, gold nanoparticles (AuNPs) based colorimetric methods have drawn considerable attention for their unique optical properties as well as the cost-efficiency and practical convenience [17–20]. The AuNPs based colorimetric methods are usually developed based on enzyme-mimic activities, interparticle cross-linking or a destabilization induced aggregation mechanism. Our group has also proposed series of AuNPs based biosensor for detection of DNA [21–23], metal ions [24,25], proteins [26,27], bioactive molecules [28,29] and cancer markers [30,31].

In this work, we developed a highly sensitive and practical colorimetric method for α-glucosidase activity assay and AGIs screening. As illustrated in Scheme 1, when AuNPs are mixed with cysteine, cysteine will be covalently immobilized onto the surface of AuNPs through the Au—S bonds. Under neutral conditions, ionization of these groups will lead to the aggregation of cysteine immobilized AuNPs due to interparticle hydrogen-bond interaction and electrostatic attraction between $—COO^-$ and $—NH_3^+$ groups [32–34]. A color change from wine red to violet can be observed. However, in the presence of iodide ions and H_2O_2, cysteine is oxidized to cystine and the oxidation product cystine cannot lead to aggregation of AuNPs [35]. In this work, maltose is used as the nature substrate of α-glucosidase to conduct our proposed sensing approach. In the presence of α-glucosidase and glucose oxidase (GOD), one molecule of maltose is sequentially hydrolyzed and oxidized to two molecules of gluconic acid and H_2O_2, respectively. So, aggregation of AuNPs will be prevented because of the oxidation of cysteine to cystine by H_2O_2. However, with the addition of AGIs, the α-glucosidase activity is inhibited and cysteine induced aggregation of AuNPs would be recovered. The employing of unmodified AuNPs provides a simple assay avoiding the involved complicated and time-consuming functional manufacture of AuNPs [36–38]. This colorimetric assay of α-glucosidase activity and inhibitor screening is simple and cost effective, which may have great potential application in the drug screening and clinical diagnose in the future.

2. Experimental

2.1. Materials

Recombinant α-glucosidase from *Saccharomyces cerevisiae* and glucose oxidase from *Aspergillusniger* (Type X-S) were purchased from Sigma–Aldrich (St. Louis, MO, USA). Gold(III) chloride trihydrate ($HAuCl_4 \cdot 3H_2O$), sodium citrate tribasic dehydrate, *N*-2-hydroxyethylpiperazine-*N*′-2-ethanesulfonic acid (HEPES), L-cysteine, potassium iodide, glucose and maltose were obtained from Sigma–Aldrich. Hydrogen peroxide (H_2O_2, 30%) and ethanol were purchased from Sinopharm Chemical Reagent Co., Ltd. (Shanghai, China). Gallic acid, quercetin and genistein were

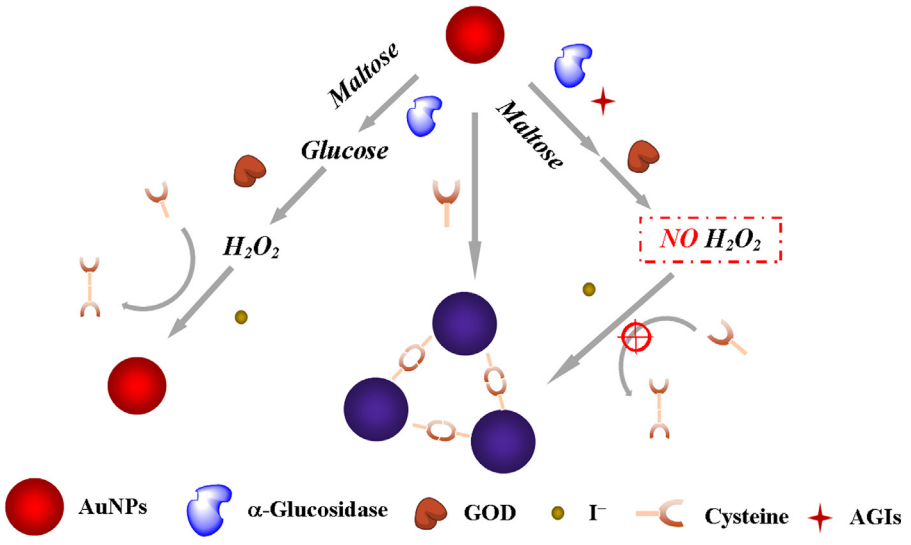

Scheme 1. Schematic illustration of the proposed method for α-glucosidase activity assay and AGIs screening.

obtained from Sigma–Aldrich. All chemicals were of analytical grade and were used as received. All aqueous solutions were prepared with deionized water purified with a Milli-Q purification system (Branstead, USA) to a specific resistance of 18 MΩ cm.

2.2. Instruments

The color changes and UV–vis absorption were recorded with a digital camera and a Shimadzu UV-2450 PC spectrophotometer (Kyoto, Japan), respectively. The measurements were conducted with a scan range from 400 nm to 800 nm. An absorbance ratio of A_{600}/A_{520} was employed to assess the aggregation of AuNPs.

2.3. Preparation of AuNPs

The 13 nm AuNPs were synthesized by the conventional citrate-reduction method [39]. Briefly, 98 mL of deionized water was added into the three-neck flask. Then 2 mL of 50 mM gold(III) solution was added with a final concentration of 1 mM. After boiling of the aqueous solution, 10 mL of 38.8 mM sodium citrate was rapidly added to the mixture with vigorous stirring under reflux condition for another 30 min. The resulting deep red solution was allowed to cool down to room temperature after additional stirring of 20 min. The AuNPs were collected by filtering through a 0.22 μm membrane, and stored free of light at 4 °C. The concentration of AuNPs was determined by recording the absorbance at 520 nm (~2.4), and using the corresponding extinction coefficient. The concentration was determined as ~13 nM.

2.4. Preparation of stock solutions

The α-glucosidase was dissolved in 50 mM HEPES (pH 7.0) with a stock concentration of 10 U mL^{-1} and placed at −20 °C [8]. Prior to solvation of GOD, 5 mL of 50 mM HEPES (pH 7.0) was purged with pure oxygen and saturated for 15 min. 250 U mL^{-1} GOD was stored at −20 °C. Unless noted, all other chemicals were dissolved in 50 mM HEPES (pH 7.0), and used with appropriate dilution. For quercetin and genistein, they were dissolved in ethanol with concentration of 1 mM due to their poor water solubility.

2.5. Detection of α-glucosidase activity and inhibition assays of AGIs

For determination of α-glucosidase activity, 5 μL of α-glucosidase with expected concentration was added into 80 μL of maltose (0.4 mM) and kept at 37 °C for time of 30 min. Then 5 μL of GOD was mixed with the solution with a final concentration of 5 U mL^{-1} under room temperature. After incubated for 30 min, the system was then reacted with 10 μL of Cys/KI mixture for another 20 min. 100 μL of AuNPs (~13 nM) was incubated with the resulting system at room temperature for the UV–vis measurement.

For the inhibition assays of AGIs, 5 μL of α-glucosidase with a fixed concentration was primarily mixed with 40 μL of different concentration of AGIs at room temperature for 20 min. Then 40 μL of maltose (0.8 mM) was added into the solution and followed with the same procedure of detection of α-glucosidase activity.

3. Results and discussion

3.1. I^-/H_2O_2 catalyzed oxidation of cysteine

The oxidation of cysteine catalyzed by I^-/H_2O_2 is attributed to the sequence of reactions outlined in Fig. 1 [35]. In the primary step, α-glucosidase and GOD catalyze the aerobic production of H_2O_2 (Eqs. (1) and (2)). The generated H_2O_2 oxidizes I^- to the intermediate IOH (Eq. (3)). RSH denotes the cysteine in Eqs. (5) and (6). Thus, RSI initiates the oxidation of thiols to disulphides (Eq. (7)). In an aerobic environment, with the constant generation of H_2O_2, an amplification cycle of the oxidation of thiol to disulfide is rolling under the essential trace level of I^- ions. Therefore, the presence of α-glucosidase leads to I^-/H_2O_2 catalyzed oxidation of cysteine to cystine in the test system.

1. $maltose + H_2O \xrightarrow{\alpha\text{-glucosidase}} glucose$
2. $glucose + O_2 + H_2O \xrightarrow{GOD} gluconic\ acid + H_2O_2$
3. $I^- + H_2O_2 \longrightarrow IOH + OH^-$
4. $IOH + I^- \longrightarrow I_2 + OH^-$
5. $IOH + RSH \longrightarrow RSI + H_2O$
6. $I_2 + RSH \longrightarrow RSI + I^- + H^+$
7. $RSI + RSH \longrightarrow RSSR + I^- + H^+$
8. $H^+ + OH^- \longrightarrow H_2O$

Fig. 1. The mechanism of I^-/H_2O_2 catalyzed oxidation of thiols to disulfides.

To verify the catalyzation of I^-/H_2O_2, we first explored the cysteine induced aggregation process of AuNPs. Fig. 2A shows the UV–vis spectra of AuNPs upon different concentration of cysteine and the related optical picture (insert). Without existence of cysteine, AuNPs display a characteristic absorption band at 520 nm. However, exogenously adding cysteine results in a concentration-depended aggregation of AuNPs. As the concentration of cysteine rising, a concomitant absorption band with increasing absorbance at 600 nm and a color change from wine red to violet of the system were observed. As shown in Fig. 2B, the concentration-depended curve presented the absorbance ratio of A_{600}/A_{520} of AuNPs upon various concentration of cysteine. An equilibrium platform is kept when the cysteine rises to a concentration of 20 μM. Thus 20 μM of cysteine was employed in this work. Then, we examined the time related effect on the aggregation process of AuNPs. Fig. 2C depicts UV–vis spectra of AuNPs with 20 μM cysteine at different times. The results reveal a progressive aggregation process. With the incremental time, an increasing absorbance at 600 nm is observed, and there is nearly no apparent increase when it arrived at the point of 30 min. Therefore, we chose the time of 30 min as the measure time for the following experiments.

As shown in Fig. 2D, the UV–vis absorption of AuNPs were observed when adding different additives. With exogenous H_2O_2 only, it was found that cysteine induced aggregation of AuNPs was conducted (Fig. 2D, green trace). Same as H_2O_2, there was no regulation of the aggregation process compared to the control group when adding I^- ions to the test solution (Fig. 2D, red trace). These results reveal that neither individual I^- ions nor H_2O_2 can generate the catalyzation of cysteine. As indicated in Fig. 1, the aggregation process is regulated only when adding both I^- ions and H_2O_2 to the system. The spectrum data verify that I^-/H_2O_2 catalyzed oxidation of cysteine to cystine inhibits the aggregation of AuNPs.

3.2. α-Glucosidase triggered oxidation of cysteine

Exogenous H_2O_2 and I^- has been proved successfully preventing the cysteine induced aggregation of AuNPs. To check the effect of endogenic enzymatic generated H_2O_2 on the aggregation process, the GOD and glucose were used. Glucose as substrate material is

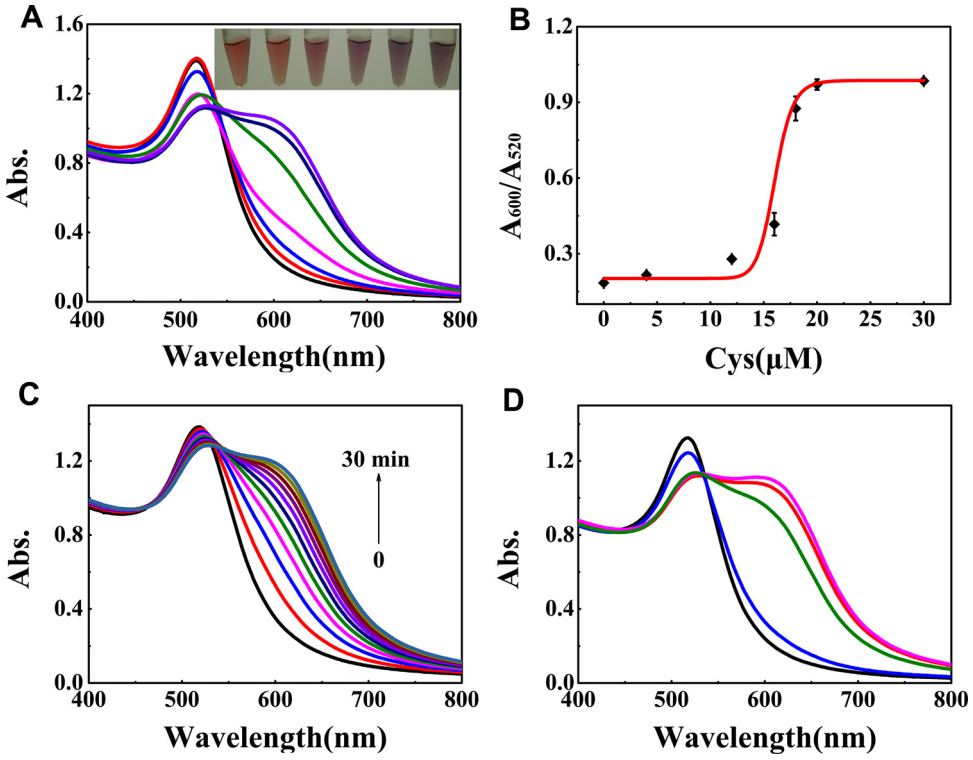

Fig. 2. (A) UV–vis absorption spectra and optical picture (insert) of AuNPs (50 mM HEPES, pH 7.0) with different concentrations of cysteine. Absorbance from low to high at 600 nm: 0.0, 4.0, 12, 16, 18, 20, 30 μM. (B) Calibration curve of the corresponding A_{600}/A_{520} absorbance ratio of AuNPs with different concentrations of cysteine. (C) Time-dependent UV–vis absorption spectra of AuNPs (50 mM HEPES, pH 7.0) upon 20 μM cysteine with a time interval of 3 min. (D) UV–vis absorption spectra of AuNPs (50 mM HEPES, pH 7.0) upon different additives after incubation. The black trace: AuNPs alone; blue trace: 0.4 μM KI, 100 μM H_2O_2, 20 μM cysteine; green trace: 100 μM H_2O_2, 20 μM cysteine; red trace: 0.4 μM KI, 20 μM cysteine; pink trace: 20 μM cysteine. (For interpretation of the references to color in this figure legend, the reader is referred to the web version of this article.)

oxidized by GOD with product of H_2O_2. The spectra (Fig. 3A) demonstrate that the absorbance band at 600 nm is vanished and the color of the system is recovered to wine red, which indicates the endogenic H_2O_2 deriving from GOD/glucose carries out a prevention to the aggregation process. The absorbance ratio histogram (Fig. 3B) depicts neither GOD nor glucose alone has a disturbance on the aggregation of AuNPs. Above results verify that endogenic enzymatic generated H_2O_2 would generate a catalyzation of cysteine to cystine and positively protect AuNPs from aggregation.

Next, α-glucosidase and its substrate maltose were applied to the system. As shown in Fig. 3, the aggregation of AuNPs was observed when α-glucosidase or maltose was added into the test system, respectively. However, the spectrum shows no absorption band at 600 nm and the absorbance ratio of A_{600}/A_{520} is similar to the control group level when adding α-glucosidase and maltose simultaneously, which verifies the α-glucosidase triggered oxidation of cysteine to cystine. Therefore, a colorimetric α-glucosidase sensing has been realized by analyzing the color changes and absorbance ratio of A_{600}/A_{520}.

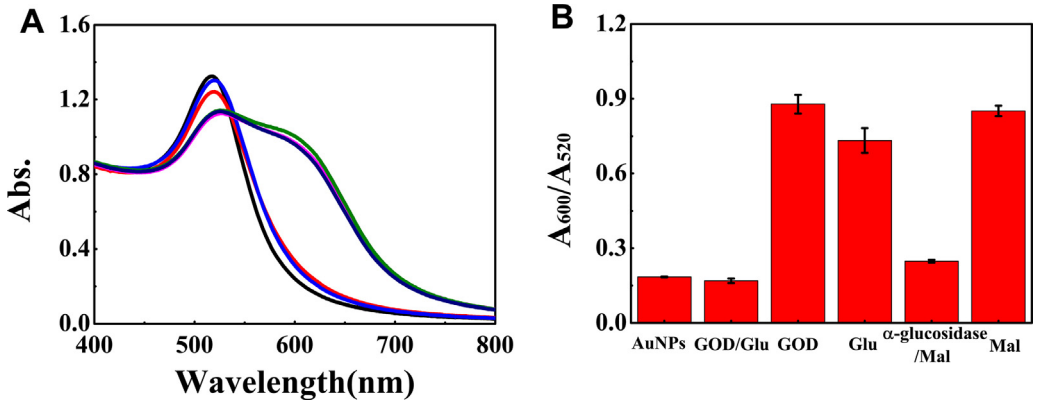

Fig. 3. (A) UV–vis absorption spectra and (B) the related A_{600}/A_{520} absorbance ratio histogram of system (50 mM HEPES, pH 7.0, 0.4 μM KI, 20 μM cysteine) response to different additives. The black trace: AuNPs alone; blue trace: 0.2 mM glucose, 5 U mL^{-1} GOD; red trace: 0.4 mM maltose, 0.05 U mL^{-1} α-glucosidase, 5 U mL^{-1} GOD; purple trace: 0.2 mM glucose; pink trace: 5 U mL^{-1} GOD; green trace: 0.4 mM maltose, 5 U mL^{-1} GOD. The error bars represent the standard derivation of three measurements conducted at each time. (For interpretation of the references to color in this figure legend, the reader is referred to the web version of this article.)

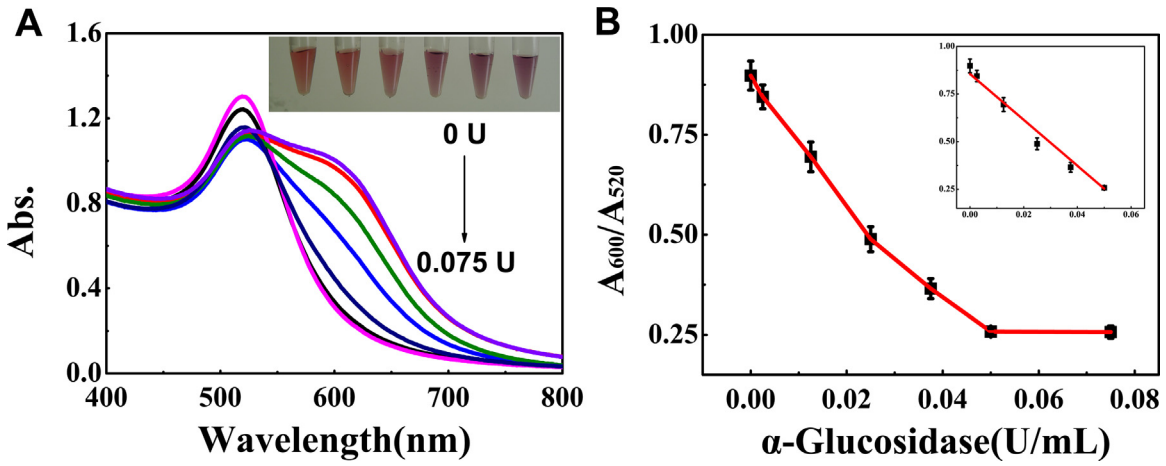

Fig. 4. (A) UV–vis absorption spectra and the related optical images of the system (50 mM HEPES, pH 7.0, 0.4 mM maltose, 5 U mL^{-1} GOD, 0.4 μM KI, 20 μM cysteine) corresponding to the detection of α-glucosidase activity at different concentrations. Low-to-high: 0, 0.0025, 0.0125, 0.025, 0.0375, 0.05, 0.075 U mL^{-1}. (B) Concentration-dependent curve corresponding to the sensing of different amount of α-glucosidase according to Scheme 1. Insert: linear fitted curve presenting the A_{600}/A_{520} absorbance ratio at different concentration of α-glucosidase in the range of 0.0025–0.05 U mL^{-1}. The error bars represent the standard derivation of three measurements conducted at each time.

3.3. α-Glucosidase activity assay

Fig. 4A shows the UV–vis spectra and optical picture of the test system upon different amount of α-glucosidase. The spectra display a decreasing absorbance band at 600 nm while the concentration of α-glucosidase rises. And the color of the system increasingly changes from violet to wine red. The concentration depended curve (Fig. 4B) demonstrates the decreasing A_{600}/A_{520} absorbance ratio until the amount of α-glucosidase up to 0.05 U mL^{-1}. A well linear relation is presented in a range of 0.0025–0.05 U mL^{-1} (Fig. 4B, insert). The detection limit of the sensor is found to be 0.001 U mL^{-1}, which is more sensitive than other reports (Table 1).

3.4. AGIs screening

Since the natural plant extracts as AGIs have drawn great interests of the potential applications as supplements or specific drugs. A well accepted concept is that the consumption of plant-based foods or supplements may be a more acceptable source of glucosidase inhibitors due to their low cost and relative safety, including a low incidence of serious gastrointestinal side effects [40–42]. Therefore, for the inhibition assay of α-glucosidase, we primarily employed acarbose as the positive control. Then, inhibition assays are conducted using three species of plant extracts which are gallic acid, quercetin and genistein. To evaluate the inhibitory effects, 0.05 U mL^{-1} α-glucosidase was employed for the inhibition analyzing due to its well regulative effect on the aggregation process of AuNPs. Three species of plant extracts (gallic acid, quercetin and genistein) were compared with a commercial available acarbose standard in this inhibition assays. Fig. 5 shows the spectra of system upon different amount of the four kinds of AGIs. In case of acarbose (Fig. 5A), no aggregation of AuNPs is observed under 0 μM acarbose. However, with the increasingly adding acarbose into the system, α-glucosidase is inactivated gradually, thus, I^-/H_2O_2 catalyzed oxidation of cysteine to cystine is blocked due to the lack of sufficient H_2O_2. Consequentially, the cysteine induced aggregation of AuNPs is carried out. The spectra depict the rising absorption band at 600 nm. Also, a color change from wine red to violet was observed progressively (insert). For the other three species, the parallel phenomena were found as well (Fig. 5B–D).

$$I = \frac{(A_{T600}/A_{T520}) - (A_{O600}/A_{O520})}{(A_{t600}/A_{t520}) - (A_{O600}/A_{O520})} \quad (9)$$

Eq. (9) was employed to quantitatively assess the inhibitory abilities, where A_t and A_O represent the absorbance of system with and without adding α-glucosidase (50 mM HEPES, pH 7.0, 0.4 mM maltose, 5 U mL^{-1} GOD, 20 μM Cys 0.4 μM KI), respectively. And A_T stands for absorbance of the system (0.05 U mL^{-1} α-glucosidase) upon different amount of AGIs. As shown in Fig. 5E, acarbose as positive control displays a strong inhibitory effect on α-glucosidase activity with an IC_{50} of 5.87 μM, which is analogical to that reported in literatures [43–45]. This result reveals I^-/H_2O_2 catalyzed oxidation of cysteine system has a sensitive response to the α-glucosidase inhibitor. Quercetin inhibition assays also shows a similar phenomenon with a slightly enlarged IC_{50} of 9.12 μM compared to acarbose. The IC_{50} values obtained applying this system for genistein is about 1.40 μM, which is lower than acarbose indicating a more efficient inhibition than others. In

Table 1
Sensor platform for α-glucosidase activity detection.

Target	Method	System	Detection limit (U mL^{-1})
α-Glucosidase	Fluorescence	Conjugated polymer and PNPG [11]	0.01
	Absorption	This study	0.001
β-Glucosidase	Absorption	Cellobiose–AuNPs complex and MCH [46]	1.0
	Absorption	Glc–Lip–AuNPs complex [37]	~2.6 (9.8 nM)
α-Amylase	Electrochemistry	Maltopentaose and $[Ru(NH_3)_5Cl]^{2+}$ [47]	0.022
	Fluorescence	CdS nanoparticle-sol–gel-thin films [48]	~3.8 (57 fM)

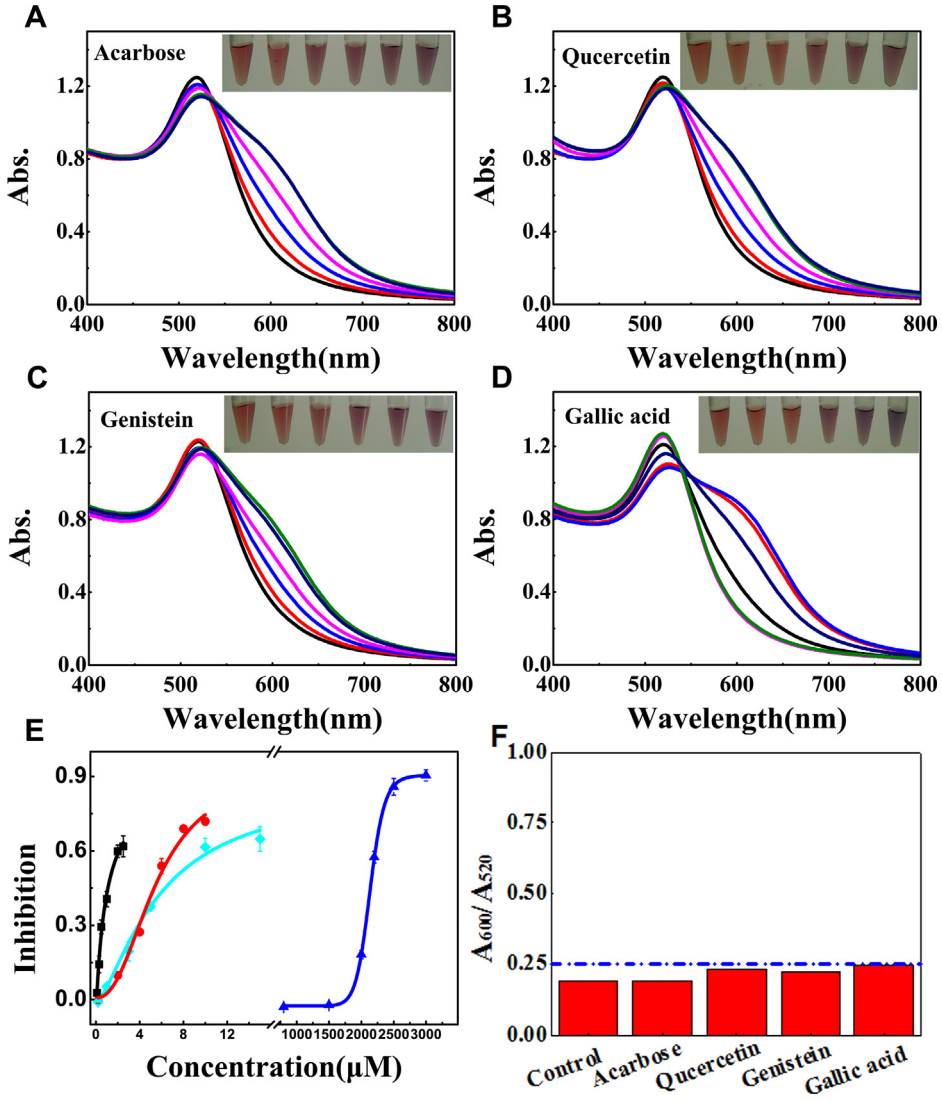

Fig. 5. (A–D) UV–vis absorption spectra and the related optical images of the system (50 mM HEPES, pH 7.0, 0.05 U mL^{-1} α-glucosidase, 0.4 mM maltose, 5 U mL^{-1} GOD, 0.4 μM KI, 20 μM cysteine) involve to the analysis of the inhibitory effects of AGIs. Absorbance from low to high at 600 nm, acarbose (A) 0.2, 2.0, 4.0, 6.0, 8.0, 10 μM; quercetin (B) 0.2, 1.0, 3.0, 5.0, 10, 15 μM; genistein (C) 0.1, 0.3, 0.5, 1.0, 2.0, 2.5 μM; gallic acid (D) 0.8, 1.5, 2.0, 2.2, 2.5, 3.0 mM. (E) Calibration curve presenting the inhibitory ability of the AGIs studied above at different concentrations. For genistein (black line), acarbose (red line), quercetin (cyan line) and gallic acid (blue line). The error bars represent the standard derivation of three measurements conducted at each time. (F) The A_{600}/A_{520} absorbance ratio histogram of the citrate-capped AuNPs response to the AGIs alone at different concentrations. For acarbose, quercetin and genistein, the concentration is 100 μM, and for gallic acid it is 5 mM, respectively. (For interpretation of the references to color in this figure legend, the reader is referred to the web version of this article.)

addition, gallic acids carry out a weakest inhibitory performance with the IC_{50} value of 2.15 mM which is far higher than the other three species obtained with this system. These results are consistent with the phenomenon reported by others. Besides, in the presence of 0.4 mM maltose, when the AGIs were mixed with AuNPs alone there was no drastic fluctuations on the UV–vis absorption properties observed (Fig. 5F). This indicates the aggregation of AuNPs is caused by the inactivation of α-glucosidase with AGIs and not a direct consequence resulting from the interference by the AGIs themselves. Therefore, the novel sensor based on the enzymatic regulation of aggregation of AuNPs provides a reliable and sensitive sensing approach. It is potential to screen new α-glucosidase inhibitors sensitively with great convenience.

4. Conclusions

In summary, we have developed a novel sensor to detect α-glucosidase activity and screen its inhibitors sensitively. The cysteine induced aggregation of AuNPs is prevented in the presence of α-glucosidase. With the addition of AGIs into the test solution, the aggregation of AuNPs is recovered with an increasing absorbance at 600 nm and the solution's color changes from wine red to violet. The detection limit for α-glucosidase is 0.001 U mL^{-1}, which is more sensitive than other reports. Attribute to its sensitivity and simplity, this new developed sensor may provide a novel platform for the detection of other enzymes and its inhibitors screening.

Acknowledgement

This work is supported by the National Natural Science Foundation of China (Grant Nos. 61275085 and 31100560).

References

[1] R.R. Koski, Practical review of oral antihyperglycemic agents for type 2 diabetes mellitus, Diabetes Educ. 32 (2006) 869–876.

[2] A. Keech, R.J. Simes, P. Barter, J. Best, R. Scott, M.R. Taskinen, P. Forder, A. Pillai, T. Davis, P. Glasziou, P. Drury, Y.A. Kesaniemi, D. Sullivan, D. Hunt, P. Colman, M. d'Emden, M. Whiting, C. Ehnholm, M. Laakso, F.S. Investigators, Effects of long-term fenofibrate therapy on cardiovascular events in 9795 people with type 2 diabetes mellitus (the FIELD study): randomised controlled trial, Lancet 366 (2005) 1849–1861.

[3] H.M. Colhoun, D.J. Betteridge, P.N. Durrington, G.A. Hitman, H.A.W. Neil, S.J. Livingstone, M.J. Thomason, M.I. Mackness, V. Charlton-Menys, J.H. Fuller, Primary prevention of cardiovascular disease with atorvastatin in type 2 diabetes in the Collaborative Atorvastatin Diabetes Study (CARDS): multicentre randomised placebo-controlled trial, Lancet 364 (2004) 685–696.

[4] A. Akomolafe, A. Beiser, J.B. Meigs, R. Au, R.C. Green, L.A. Farrer, P.A. Wolf, S. Seshadri, Diabetes mellitus and risk of developing Alzheimer disease: results from the Framingham study, Arch. Neurol. 63 (2006) 1551–1555.

[5] F.A. van de Laar, P.L. Lucassen, R.P. Akkermans, E.H. van de Lisdonk, G.E. Rutten, C. van Weel, α-Glucosidase inhibitors for patients with type 2 diabetes: results from a cochrane systematic review and meta-analysis, Diabetes Care 28 (2005) 154–163.

[6] R. Mata, S. Cristians, S. Escandón-Rivera, K. Juárez-Reyes, I. Rivero-Cruz, Mexican antidiabetic herbs: valuable sources of inhibitors of α-glucosidases, J. Nat. Prod. 76 (2013) 468–483.

[7] W. Hakamata, M. Kurihara, H. Okuda, T. Nishio, T. Oku, Design and screening strategies for alpha-glucosidase inhibitors based on enzymological information, Curr. Top. Med. Chem. 9 (2009) 3–12.

[8] F. Brindis, R. Rodri'guez, R. Bye, M. Gonza'lez-Andrade, R. Mata, (Z)-3-Butylidenephthalide from *Ligusticum porteri*, an α-glucosidase inhibitor, J. Nat. Prod. 74 (2010) 314–320.

[9] M.-m. Si, J.-s. Lou, C.-X. Zhou, J.-N. Shen, H.-H. Wu, B. Yang, Q.-J. He, H.-S. Wu, Insulin releasing and alpha-glucosidase inhibitory activity of ethyl acetate fraction of *Acorus calamus* in vitro and in vivo, J. Ethnopharmacol. 128 (2010) 154–159.

[10] Z. Yu, Y. Yin, W. Zhao, Y. Yu, B. Liu, J. Liu, F. Chen, Novel peptides derived from egg white protein inhibiting alpha-glucosidase, Food Chem. 129 (2011) 1376–1382.

[11] A. Cao, Y. Tang, Y. Liu, Novel fluorescent biosensor for α-glucosidase inhibitor screening based on cationic conjugated polymers, ACS Appl. Mater. Interfaces 4 (2012) 3773–3778.

[12] Y. Sawada, T. Tsuno, T. Ueki, H. Yamamoto, Y. Fukagawa, T. Oki, Pradimicin-Q, a new pradimicin aglycone, with alpha-glucosidase inhibitory activity, J. Antibiot. 46 (1993) 507–510.

[13] Y. Zhang, G.-M. Zeng, L. Tang, D.-L. Huang, X.-Y. Jiang, Y.-N. Chen, A hydroquinone biosensor using modified core–shell magnetic nanoparticles supported on carbon paste electrode, Biosens. Bioelectron. 22 (2007) 2121–2126.

[14] Y. Zhang, G.-M. Zeng, L. Tang, Y.-P. Li, L.-J. Chen, Y. Pang, Z. Li, C.-L. Feng, G.-H. Huang, An electrochemical DNA sensor based on a layers-film construction modified electrode, Analyst 136 (2011) 4204–4210.

[15] Y. Zhang, G.-M. Zeng, L. Tang, Y.-P. Li, Z.-M. Chen, G.-H. Huang, Quantitative detection of trace mercury in environmental media using a three-dimensional electrochemical sensor with an anionic intercalator, RSC Adv. 4 (2014) 18485–18492.

[16] Y. Zhang, G.M. Zeng, L. Tang, J. Chen, Y. Zhu, X.X. He, Y. He, Electrochemical sensor based on electrodeposited graphene-Au modified electrode and nanoAu carrier amplified signal strategy for attomolar mercury detection, Anal. Chem. 87 (2014) 989–996.

[17] S. Lee, E.-J. Cha, K. Park, S.-Y. Lee, J.-K. Hong, I.-C. Sun, S.Y. Kim, K. Choi, I.C. Kwon, K. Kim, C.-H. Ahn, A near-infrared-fluorescence-quenched gold-nanoparticle imaging probe for in vivo drug screening and protease activity determination, Angew. Chem. Int. Ed. 47 (2008) 2804–2807.

[18] X. Xu, M.S. Han, C.A. Mirkin, A gold-nanoparticle-based real-time colorimetric screening method for endonuclease activity and inhibition, Angew. Chem. Int. Ed. 46 (2007) 3468–3470.

[19] I.H. El-Sayed, X. Huang, M.A. El-Sayed, Surface plasmon resonance scattering and absorption of anti-EGFR antibody conjugated gold nanoparticles in cancer diagnostics: applications in oral cancer, Nano Lett. 5 (2005) 829–834.

[20] Y. Cheng, A.C. Samia, J.D. Meyers, I. Panagopoulos, B. Fei, C. Burda, Highly efficient drug delivery with gold nanoparticle vectors for in vivo photodynamic therapy of cancer, J. Am. Chem. Soc. 130 (2008) 10643–10647.

[21] X. Zhu, Y. Liu, J. Yang, Z. Liang, G. Li, Gold nanoparticle-based colorimetric assay of single-nucleotide polymorphism of triplex DNA, Biosens. Bioelectron. 25 (2010) 2135–2139.

[22] Q. Fan, J. Zhao, H. Li, L. Zhu, G. Li, Exonuclease III-based and gold nanoparticle-assisted DNA detection with dual signal amplification, Biosens. Bioelectron. 33 (2012) 211–215.

[23] Y. Yang, C. Li, L. Yin, M. Liu, Z. Wang, Y. Shu, G. Li, Enhanced charge transfer by gold nanoparticle at DNA modified electrode and its application to label-free DNA detection, ACS Appl. Mater. Interfaces 6 (2014) 7579–7584.

[24] H. Chen, J. Zhang, X. Liu, Y. Gao, Z. Ye, G. Li, Colorimetric copper(II) ion sensor based on the conformational change of peptide immobilized onto the surface of gold nanoparticles, Anal. Methods 6 (2014) 2580–2585.

[25] C. Li, L. Wei, X. Liu, L. Lei, G. Li, Ultrasensitive detection of lead ion based on target induced assembly of DNAzyme modified gold nanoparticle and graphene oxide, Anal. Chim. Acta 831 (2014) 60–64.

[26] T. Liu, J. Zhao, D. Zhang, G. Li, Novel method to detect DNA methylation using gold nanoparticles coupled with enzyme-linkage reactions, Anal. Chem. 82 (2009) 229–233.

[27] Y. Xu, J. Wang, Y. Cao, G. Li, Gold nanoparticles based colorimetric assay of protein poly(ADP-ribosyl) ation, Analyst 136 (2011) 2044–2046.

[28] X. Zhu, Q. Yang, J. Huang, I. Suzuki, G. Li, Colorimetric study of the interaction between gold nanoparticles and a series of amino acids, J. Nanosci. Nanotechnol. 8 (2008) 353–357.

[29] C. Li, Y. Yang, B. Zhang, G. Chen, Z. Wang, G. Li, Conjugation of graphene oxide with DNA-modified gold nanoparticles to develop a novel colorimetric sensing platform, Part. Part. Syst. Charact. 31 (2014) 201–208.

[30] J. Wang, Y. Cao, Y. Xu, G. Li, Colorimetric multiplexed immunoassay for sequential detection of tumor markers, Biosens. Bioelectron. 25 (2009) 532–536.

[31] H. Xie, H. Li, Y. Huang, X. Wang, Y. Yin, G. Li, Combining peptide and DNA for protein assay: CRIP1 detection for breast cancer staging, ACS Appl. Mater. Interfaces 6 (2013) 459–463.

[32] E. Sharon, E. Golub, A. Niazov-Elkan, D. Balogh, I. Willner, Analysis of telomerase by the telomeric hemin/G-quadruplex-controlled aggregation of Au nanoparticles in the presence of cysteine, Anal. Chem. 86 (2014) 3153–3158.

[33] F. Wang, X. Liu, C.-H. Lu, I. Willner, Cysteine-mediated aggregation of Au nanoparticles: the development of a H2O2 sensor and oxidase-based biosensors, ACS Nano 7 (2013) 7278–7286.

[34] J. Wang, Y.F. Li, C.Z. Huang, T. Wu, Rapid and selective detection of cysteine based on its induced aggregates of cetyltrimethylammonium bromide capped gold nanoparticles, Anal. Chim. Acta 626 (2008) 37–43.

[35] M. Kirihara, Y. Asai, S. Ogawa, T. Noguchi, A. Hatano, Y. Hirai, A mild and environmentally benign oxidation of thiols to disulfides, Synthesis 21 (2007) 3286–3289.

[36] J. Zhang, Y. Liu, J. Lv, G. Li, A colorimetric method for α-glucosidase activity assay and its inhibitor screening based on aggregation of gold nanoparticles induced by specific recognition between phenylenediboronic acid and 4-aminophenyl-α-D-glucopyranoside, Nano Res. 7 (2014) 1–11.

[37] Z. Zeng, S. Mizukami, K. Kikuchi, Simple and real-time colorimetric assay for glycosidases activity using functionalized gold nanoparticles and its application for inhibitor screening, Anal. Chem. 84 (2012) 9089–9095.

[38] C.-J. Kim, D.-I. Lee, C. Kim, K. Lee, C.-H. Lee, I.-S. Ahn, Gold nanoparticles-based colorimetric assay for cathepsin B activity and the efficiency of its inhibitors, Anal. Chem. 86 (2014) 3825–3833.

[39] J. Liu, Y. Lu, Preparation of aptamer-linked gold nanoparticle purple aggregates for colorimetric sensing of analytes, Nat. Protoc. 1 (2006) 246–252.

[40] W. Benalla, S. Bellahcen, M. Bnouham, Antidiabetic medicinal plants as a source of alpha glucosidase inhibitors, Curr. Diabetes Rev. 6 (2010) 247–254.

[41] O. Said, S. Fulder, K. Khalil, H. Azaizeh, E. Kassis, B. Saad, Maintaining a physiological blood glucose level with 'glucolevel', a combination of four anti-diabetes plants used in the traditional Arab herbal medicine, Evid. Based Complement. Altern. Med. 5 (2008) 421–428.

[42] M. Yilmazer-Musa, A.M. Griffith, A.J. Michels, E. Schneider, B. Frei, Grape seed and tea extracts and catechin 3-gallates are potent inhibitors of α-amylase and α-glucosidase activity, J. Agric. Food Chem. 60 (2012) 8924–8929.

[43] J.-S. Kim, T.K. Hyun, M.-J. Kim, The inhibitory effects of ethanol extracts from sorghum, foxtail millet and proso millet on α-glucosidase and α-amylase activities, Food Chem. 124 (2011) 1647–1651.

[44] C. Hansawasdi, J. Kawabata, T. Kasai, Hibiscus acid as an inhibitor of starch digestion in the caco-2 cell model system, Biosci. Biotechnol. Biochem. 65 (2001) 2087–2089.

[45] M.S. Deutschländer, N. Lall, M. Van de Venter, A.A. Hussein, Hypoglycemic evaluation of a new triterpene and other compounds isolated from *Euclea undulata* Thunb. var. myrtina (Ebenaceae) root bark, J. Ethnopharmacol. 133 (2011) 1091–1095.

[46] C. Lai, G.-M. Zeng, D.-L. Huang, M.-H. Zhao, M. Chen, Z. Wei, C. Huang, P. Xu, N.-J. Li, X. Li, C. Zhang, Colorimetric screening of β-glucosidase inhibition based on gold nanocomposites, Anal. Methods 6 (2014) 312–315.

[47] J. Zhang, J. Cui, Y. Liu, Y. Chen, G. Li, A novel electrochemical method to determine α-amylase activity, Analyst 139 (2014) 3429–3433.

[48] M.S. Attia, H. Zoulghena, M.S.A. Abdel-Mottaleb, A new nano-optical sensor thin film cadmium sulfide doped in sol–gel matrix for assessment of β-amylase activity in human saliva, Analyst 139 (2014) 793–800.